P8.11   GLOBAL RETRIEVALS OF THE SURFACE AND ATMOSPHERE RADIATION BUDGET AND DIRECT AEROSOL FORCING

Thomas P. Charlock[1], Fred G. Rose[2], David Rutan[2], Zhonghai Jin[2], David Fillmore[3], and William Collins[3]

[1] NASA Langley Research Center, Hampton, VA

[2] Analytical Services & Materials Inc., Hampton, VA

[3] NCAR, Boulder, CO

1 INTRODUCTION

This document describes the retrieval of the vertical profiles of radiative fluxes with CERES Terra data CRS Edition 2A (sections 2-7); an official publically available product. We then give a brief off line test of the radiative transfer algorithm with observations from the Cheseapeake Lighthouse and Aircraft Measurements for Satellites (CLAMS) field campaign. (section 8); the test includes a diagnosis of the direct forcing of aerosols with the code. A companion paper by Rutan et al., (2004) explains the validation of the retrieved fluxes at the surface. CERES (Wielicki et al., 1997) is a complex program that observes broadand radiative fluxes, retrieves clouds and aerosols, and then also computes fluxes. CERES operates on the TRMM, Terra, and Aqua spacecraft. Examples of retrieval of profiles of fluxes, intensive records of ground-based measurements for validation, systematic comparisons of retrievals with measurements, and "point and click" versions of the radiative transfer codes used here are found at the URL http://www-cave.larc.nasa.gov/cave/

2 DESCRIPTION OF THE CERES SURFACE AND ATMOSPHERE RADIATION PRODUCT (SARB)
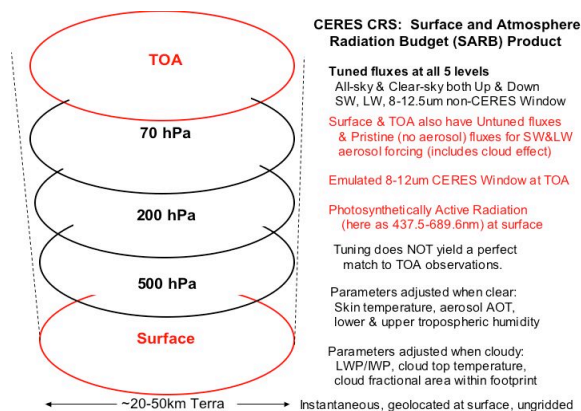

Figure 1 CERES Surface and Atmosphere Radiation Budget (SARB) product (dubbed "CRS")

The CERES Surface and Atmospheric Radiation Budget (SARB) product (Figure 1) on the Terra spacecraft is designed for studies of the energy balance within the atmosphereas require fields of clouds, humidity and aerosol that are consistent with radiative fluxes from the surface to the Top Of the Atmosphere (TOA). Like its parent database dubbed Single Scanner Footprint (SSF), SARB corresponds to an instantaneous CERES broadband footprint. The footprint has nominal nadir resolution of 20 km for half power points but is larger at other view angles (Figure 2).
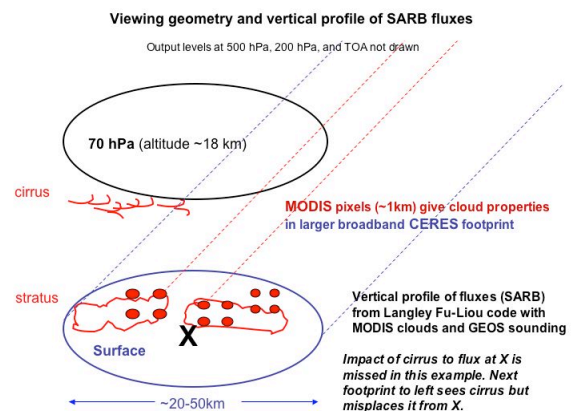

Figure 2: Typical viewing geometry showing small MODIS pixels within large CERES footprints; dimensions are roughly to scale.

Corresponding Author:
Thomas P. Charlock (Thomas.P.Charlock@nasa.gov)
Mail Stop 420
NASA Langley Research Center
Hampton, Virginia 23681

Input data for computing SARB vertical profile at ~2,000,000 footprints/day

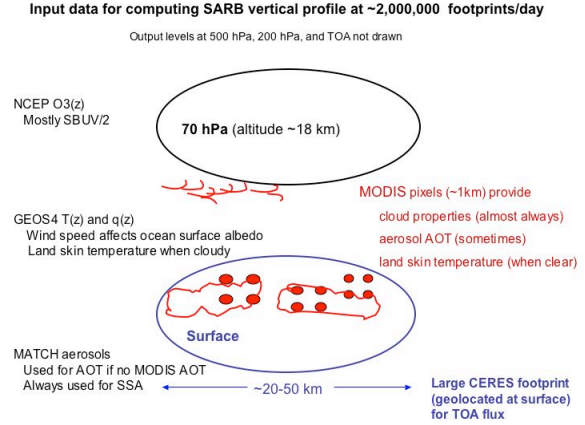Output levels at 500 hPa, 200 hPa, and TOA not drawn

Figure 3. Inputs for determining the Surface and Atmosphere Radiation Budget (SARB)

The major inputs (Figure 3) to the SARB software are the instantaneous scene identification, cloud and aerosol properties from the MODIS cloud imager pixels (resolution ~1 km), and TOA radiation (from the CERES instrument) contained on the respective SSF footprint; along with 6-hourly gridded fields of temperature, humidity, wind, and ozone, and climatological aerosol data contained on the Meteorological, Ozone, and Aerosol (MOA) internal file. MOA includes meteorological data provided by GEOS4 and the Stratospheric Monitoring Group Ozone Blended Analysis (SMOBA, Yang et al., 2000) ozone profiles from NCEP. Aerosol information is taken from MODIS and from the NCAR Model for Atmospheric Transport and Chemistry (MATCH, an assimilation that here also employs aerosol retrievals from AVHRR, Collins et al. 2001). The CERES SARB consists of through-the-atmosphere radiative flux profiles calculated by algorithms that partially constrain to CERES TOA observations; adjustments to key input parameters (i.e., optical depth for cloudy footprints and skin temperature for clear footprints); and diagnostic parameters. SARB fluxes are produced for shortwave (SW), longwave (LW), the 8.0-12.0 μm window (WN), both upwelling and downwelling at TOA, 70 hPa, 200 hPa, 500 hPa, and the surface (Figure 3). To permit the user to infer cloud forcing and direct aerosol forcing, we include surface and TOA fluxes that have been computed for cloud-free (clear) and aerosol-free (pristine) footprints; this accounts for aerosol effects (SW and LW) to both clear and cloudy skies. We refer to an earlier CERES SARB record from the low-latitude TRMM spacecraft: Charlock et al. (2002) compare time series of computed fluxes at TOA with CERES observations and illustrate how the flux profiles are related to the

tropical circulation. Rutan et al. (2002) point out that the present results do not support "anomalous absorption" of SW by clouds. Rose and Charlock (2002) note further advances in the radiative transfer code which are used in this Terra product (but not in TRMM).

3. CONSTRAINMENT (TUNING)

In short, the SARB flux profile in the CRS product is the output of a highly modified Fu and Liou (1993) radiative transfer code. The code is run at least twice for each broadband CERES footprint, in order to adjust inputs that determine the vertical profile of radiative fluxes. The constrainment (or tuning) algorithm does NOT yield a perfect match to CERES broadband observations at TOA. Constrainment (Rose et al. 1997; Charlock et al. 1997) is an approach to minimize the normalized, least squares differences between (1) computed TOA parameters and adjusted values for key inputs and (2) observed TOA parameters and initial values for key inputs. The algorithm assigns an a priori numerical "sigma" (uncertainty) to each TOA parameter and key input parameter. The "sigmas" for TOA parameters (first group in Table 1) are the anticipated rms differences between observations based on the core CERES instrument and the outputs of radiative transfer calculations. The sigmas for key input parameters (the second and third groups labeled "cloud" and "other" in Table 1) are the anticipated rms differences between the initial (untuned) and final values of those key input parameters (tuned).

Table 1: The a priori uncertainty ("sigma") for each adjustable parameter in the constrainment (tuning)

algorithm that produces the Surface and Atmosphere Radiation Budget (SARB) for CERES footprints

Observed by CERES at TOA (SSF record)			
	Sigma (%)	Minimum sigma (MKS)	Parameter
TOA	1.0 %	2.0 Wm^{-2}	reflected SW flux
	1.0 %	2.0 Wm^{-2}	broadband LW flux
	2.0 %	1.0 Wm^{-2}	window WN flux
	5.0 %	0.3 Wm^{-2} sr^{-1}	broadband LW radiance
	5.0 %	0.3 Wm^{-2} sr^{-1}	filtered window radiance

From MODIS imager (SSF record)		
	Sigma	Adjustable parameter
Cloud	0.15	d ln(tau)= optical depth
	2.0	cloud top temperature
	0.05	total cloud fraction in footprint
	0.025	fraction swap of 2 cloud types in footprin (i.e., increase Cu and decrease Ci)

From various sources			
	Ocean	Land	Adjustable parameter
Other	1.0 K	4.0 K	surface skin temperature
	0.15	0.10	d ln(PW) PW: surface to 500 hPa
	0.15	0.10	d ln(UTH) upper tropos. humidity
	0.002	0.015	surface albedo
	0.50	0.10	d ln(tau) aerosol optical depth

The inputs for radiative transfer calculations are depicted in Figure 3. The initial values of cloud parameters are taken from the SSF; they are narrowband imager-based retrievals of cloud properties. Initial values of other key input parameters such as PW and UTH are based on GEOS4. Aerosol information is taken from MODIS when available for the instantaneous CERES footprints. If the MODIS instanteneous AOT is not available for the footprint, we interpolate AOT from a file of the MODIS Daily Gridded Aerosol for the calendar month of processing. When cloudiness in the footprint exceeds 50%, or when there is no MODIS AOT, we use AOT from the NCAR Model for Atmospheric Transport and Chemistry (MATCH).

4 RADIATIVE TRANSFER

CERES geophysical products define SW (shortwave or solar) and LW (longwave or thermal infrared) in terms of physical origin, rather than wavelength. We refer to the solar energy which enters and exits (overwhemingly by reflection) the earth-atmosphere system as SW. LW is regarded as the thermal energy which is emitted by the earth-atmosphere system. There is no wavelength of demarcation, for which all radiation at shorter (longer) wavelengths is called SW (LW). Thus defined, roughly 1% of the incoming SW is at wavelengths longer than 4 μs. A small amount of radiation from the sun enters the troposphere at 10 μs. This too is regarded as SW, and we strive to account for it in successive SW products. Less than 1 Wm^{-2} of OLR is at wavelengths below 4 μs. If the radiation was originally emitted by a thermal process in the earth-atmosphere system, we regard it as LW, even if it is subsequently scattered. When a small amount of thermal radiation is emitted from the surface of the Sahara at 6 μs, and a portion of that is scattered upward to space through a cirrus cloud, said portion is regarded as LW. The 8.0-12.0 μm window (WN) products are a repository of the thermal radiation in the window. We strive to eliminate any signal of solar contamination in an 8.0-12.0 μm window or broadband LW product.

The official CERES window (WN) spans 8.0 μm to 12.0 μm (1250 cm^{-1} to 833.333 cm^{-1}). The TOA observed SSF window products use this interval, as do the TOA emulated window product. CRS users should be aware that the vertical profiles of window flux use a DIFFERENT spectral interval, 8.0 μm to 12.5 μm (1250 cm^{-1} to 800 cm^{-1}), as explained in the next section.

CRS uses a fast, plane parallel correlated-k radiative transfer code (Fu and Liou, 1993, Fu et al., 1998, 1999) which has been highly modified. It is referred to as the "Langley Fu-Liou code". An economical 2 stream calculation is used for SW. The LW calculation employs a 2/4 stream version, wherein the source function is evaluated with the quick 2-stream approach, while radiances are effectively computed at 4 streams. Constituents for the thermal infrared include H2O, CO2, O3, CH4 and N2O. A special treatment of the CERES 8.0-12.0 μm window includes CFCs (Kratz and Rose, 1998) and uses the Clough CKD 2.4 version of the H2O continuum (the orginial Fu-Liou employed the Roberts continuum). In collaboration with Dr. Qiang Fu, the Fu-Liou code was modified to include 10 separate bands between

0.2-0.7 µs to better account for the interaction of Rayleigh scattering, aerosols, and absorption by O3 and a minor band of H2O. In cooperation with Dr. Seiji Kato,, we have included the HITRAN2000 data base for the determination of correlated k's in the SW (Kato et al., 1999). We make a first order accounting for the inhomogeneity of cloud optical thickness (using the gamma weighted two stream approximation of Kato et al., 2004) in the SW, fitting the 13-element SSF histogram of cloud optical thickness with a gamma distribution. The original code included SW from 0.2 to 4 µs. In addition, we cover the SW at wavelengths larger than 4 µs by simply stuffing the solar insolation beyond 4 µm into a near IR band with strong absorption by H2O. Downwelling solar photons larger than 4 µs are then mostly absorbed by the model before reaching the middle troposphere. Scattering by cloud particles, aerosols, and a non-black surface is parameterized in LW, as well as SW. For example, the desert surface has reduced thermal emission as it is non-black. As its emissivity is less than unity, the reduction in upward LW emitted by the surface is partly compensated by reflection of the downwelling LW to the surface. The code has been extended with a new band to cover thermal emission from 2200-2850 cm^{-1}.

The Fu-Liou code covers the window with 3 bands from 8.0 µm to 12.5 µm (1250 cm^{-1} to 800 cm^{-1}); vertical profiles of window flux use this interval. A different window interval, 8.0 µm to 12.0 µm (1250 cm^{-1} to 833.333 cm^{-1}), is used for TOA observations on SSF and for the formal TOA emulations. The 8.0 µm to 12.0 µm TOA window parameters on SSF are emulated (modeled) as follows with the Langley Fu-Liou code. First, the code produces window radiance and flux for 8.0 µm to 12.5 µm at TOA; the modeled

radiance and flux constitute a theoretical Angular Distribution Model (ADM relating radiance to flux) for the footprint. Second, a straightforward parameterization based on MODTRAN4 (Anderson et al.) is then applied; the inputs are view zenith angle and radiance. The parameterization maps the 8.0 µm to 12.5 µm Fu-Liou radiance to an "unfiltered" (geophysical) 8.0 µm to 12.0 µm emulated radiance and also to a "filtered" 8.0 to 12.0 µm emulated radiance. Recall that the spacecraft itself observes a filtered radiance, a signal which includes the effect of the spectral response of the instrument. It is the task of SSF to account for the spectral response and produce an unfiltered radiance. In the second step here, the spectral response (filter function) of the instrument is modeled, producing an emulated filtered window radiance. Third, the theoretical ADM (based on 8.0 µm to 12.5 µ) converts the unfiltered 8.0 µto 12.0 µm emulated radiance into an emulated window flux. The unfiltered, emulated window radiance is not archived.

While the original Fu-Liou code offered empirical droplet size spectra based on early field campaign data, we now use theoretical, gamma distributions for the radii of cloud water droplets (Hu and Stamnes, 1994), consistent with the Minnis et al. (1998) retrievals on CERES SSF input stream. The code treats all ice cloud crystals as randomly oriented hexagons characterized by a generalized effective diameter Dge. The SSF cloud retrievals also assume randomly oriented hexagons but express them as effective diameter De. Caution is advised when interpreting CRS results for ice clouds, as both the input cloud retreivals (SSF) and the radiative transfer calculations do not account for the enormous variation of crystal shapes found in nature.

5 REFLECTION OF SW BY SURFACE

The spectral dependence of surface reflectivity for land surface albedos are specified according to the CERES Surface Properties maps (from www-surf.larc.nasa.gov/surf) following Rutan and Charlock (1997 and 1999). CRS uses the Wilber et al. (1999) surface LW spectral emissivity maps (which are available at the same URL). Both SW and LW surface maps are keyed to International Geophysical Biospherical Project (IGBP) land types. For the category of Permanent Snow and Ice, the spectral shape of reflectance is taken from a model by Jin et al. (1994) assuming 1000 µm snow grains; a grains size of 50 µm is assumed for the spectral shape

of fresh snow. The spectral shape of sea ice also employs Jin et al. (1994).

Ocean spectral albedo is obtained using a look up table (LUT) based on discrete ordinate calculations with a sophisticated coupled ocean atmosphere radiative transfer code (Jin et al., 2002, Jin and Stamnes, 1994). Inputs to the look-up table for ocean spectral albedo include cosine of the solar zenith angle (cosSZA), wind speed (from ECMWF), chlorophyll concentration (which has a minor effect on broadband flux), and SW optical depth of clouds and aerosols (from SSF) for the respective spectral interval. There is an empirical correction for surface foam based on wind speed.

For clear footprints during daytime, the broadband surface albedo is explicitly retrieved using TOA observations and iterations of the Langley Fu-Liou code with the constrainment algorithm; the broadband albedo is then simply a ratio of upwelling to downwelling SW at the surface. When a CRS footprint contains clouds, the broadband surface albedo is assumed using the Surface Albedo History (SAH) procedure. The SAH algorithm is run at the start of each month of CRS processing. SAH identifies the clear SSF footprints during the month with the most favorable geometry for the retreival of surface albedo: those with large values of cosSZA. SAH uses a quick table look-up to the Langley Fu-Liou code that relates TOA albedo, surface albedo, cosSZA, precipitable water (PW), and aerosol optical thickness (AOT). Using the footprint AOT (from MODIS or the MATCH aerosol assimilation), the look-up retrieves a first guess surface albedo for the month. This first guess surface albedo corresponds to a clear SSF/CRS footprint. The monthly value for the first guess surface albedo is then written to a SAH file for each of the 10 by 10 minute gridded tiles, whose center points are contained in the clear footprint. Each 10 by 10 minute gridded tile of land is thus given an initial broadband surface albedo for the month. The SAH albedo is stored internally as a reference value A_o using the Dickinson (1982) relationship

$$A(cosSZA) = A_o(1 + d)/(1 + 2d\ cosSZA)$$

where d is specified for each IGBP type and A_o is the albedo at cosSZA of 0.5. The look-up, first guess values of A_o for the various 10 by 10 minute tiles are then available to construct a fixed broadband surface albedo as an input for radiative transfer calculations with any cloudy footprint, for which we assume A(cosSZA=0.5). When a land footprint is clear during daylight, the surface albedo is explicitly retrieved with the CRS constrainment algorithm by iterating the code (not as a quick table look up) with GEOS4 sounding and MODIS (MOD04) and/or MATCH aerosol inputs. The quality of the surface albedo retrieval depends heavily on the realism of simulation of AOT and the CRS assignment of the corresponding single scattering albedo (see aerosol discussion and Table 2). The most reliable CRS values of surface albedo are expected for clear footprints under high sun, in regions and seasons with low AOT. Unfortunately, the CRS surface albedo retrieval for desert is not reliable, because we assume too much absorption by desert dust (see next section).

The Photosynthetically Active Radiation (PAR) product, which is generated only at the surface, is simply the SW output from 437.5 to 689.6 nm, rather than the traditional PAR interval of 400-700 nm. To date, we have not compared this non-traditional PAR with any surface observations.

6 TREATMENT OF AEROSOLS

Each footprint accounts for the effect of aerosols on SW fluxes, LW fluxes and 8.0-12.0 µm window fluxes at all levels, and on broadband LW and filtered window radiance at TOA. Aerosol information is taken from MODIS (the MODIA Atmospheres MOD04 product described by Kaufman et al., 1997) when available for the instantaneous CERES footprints. Over the ocean, MOD04 is used for 7 wavelengths; the AOT is interpolated to the remainder of the spectrum using the selected aerosol type, as specified below. Over the land, MOD04 provides AOT at 3 wavelengths, and the MOD04 Angstrom exponent is used to guide the extension over the spectrum. If the MOD04 instanteneous AOT is not available for the footprint, we temporally interpolate from a file of the MODIS Daily Gridded Aerosol as noted earlier. When cloudiness in the footprint exceeds 50%, or when there is no MODIS AOT, we use AOT from the NCAR Model for Atmospheric Transport and Chemistry (MATCH, an assimilation that here also employs MODIS, see Fillmore et al., 2004 and Collins et al., 2001). MOD04 does not span the entire globe; it does not include the cryosphere and most deserts, for example. When AOT is taken from MATCH, we assume it for one wavelength only, 0.63µm (a coding error assumed another value, but the impact is genarlly < 1%). MATCH provides AOT according to 7 types (Table 2) on a daily basis over the globe for all sky conditions. Sources of aerosol in MATCH include formation from industrial emissions (as a climatology). More timely MATCH AOT inputs include MOD04-based retreivals over clear regions; and an algorithm for wind-blown dust. MATCH itself accepts the NCEP analysis as an meteorological input. MATCH advects aerosols and removes aerosols with wet (cloudy) and dry processes. For economy in transferring MATCH files from NCAR, we take on the column AOTs of each type (rather than the profile) and assume "climatological" vertical scale heights that do not vary in space and time (Table 2).

MATCH aerosol type	CRS aerosol optics	scale height
dust (0.01-1.0μm)	dust (0.5 μm) Tegen-Lacis	3.0 km
dust (1-10 μm)	dust (2.0 μm) Tegen-Lacis	1.0 km
dust (10-20 μm)	dust (2.0 μm) Tegen-Lacis	1.0 km
dust (20-50 μm)	dust (2.0 μm) Tegen-Lacis	1.0 km
hydrophilic black carbon	soot (OPAC)	3.5 km
hydrophobic black carbon	soot (OPAC)	3.5 km
hydrophilic organic carbon	soluble organic (OPAC)	3.8 km
hydrophobic organic carbon	insoluble organic (OPAC)	3.8 km
sulfate	sulfate (OPAC)	3.5 km
sea salt	sea salt (OPAC)	0.5 km

While AOT is based on either MOD04 (a satellite retrieval) or MATCH (a model), aerosol type is always taken from MATCH. Aerosol type here guides the selection of the asymmetry factory (g) and the single scattering albedo (SSA). The spectral single scattering albedos and asymmetry factors are assumed from the Tegen and Lacis (1996) and OPACS-GADS (Hess et al., 1998; d'Almeida et al., 1991) models. Footprints with significant amounts of Tegen and Lacis 2.0 μm dust and/or OPAC soot will have strong absorption by aerosols in the computed SW. As CRS has coarse vertical resolution (i.e., outputs at surface and 500 hPa), the assignment of scale height should have a small effect on SW in most clear footprints. But if a dust outbreak spreads to say 6 km, the CRS aerosol forcing in the LW will not be realistic at either the surface or at TOA.

Recent studies with AERONET (Dubovik et al., 2002) suggest that absorption is too high in the Tegen and Lacis 2.0 μm dust. If Dubovik et al. are correct, both our computed atmospheric absorption for desert dust and our retrieved desert surface albedos would then be high, too. But dust optical depths in the MATCH assimilation are overwhelmingly of the 0.01-1.0 um class (Table 2), for which we assign the radius 0.5 μ. Single scattering albedoes for the Tegen and Lacis 0.5μm dust are closer to the values reported by Dubovik et al. Any CRS footprint containing a significant loading of desert dust will have values for computed SW fluxes that are suspect. As the surface albedo is the ratio of two computed SW fluxes, the surface albedo over deserts (i.e., the Sahara, which has much dust) is also suspect.

7 COMPARISON WITH OBSERVATIONS

CERES observations of radiances (Wm-2sr-1) at satellite altitude are reported on the SSF file, a key source for the computed radiation fields reported here as CRS. Observed broadband SW, broadband LW (OLR). and window (8-12 μm) fluxes (irradiances in Wm-2) at the top of the atmosphere (TOA) reference level are interpreted from (1) observed radiances at the respective footprints and (2) and sets of statistics at many footprints with similar charactistics (i.e., scene type and SZA). Table 3 contains "raw" statistics of fooprints from the entire globe for one day; they have not been gridded to correctly represent particular regions of the globe. Terra CRS is based on a routine subset every other (50%) of SSF footprints. The scan pattern of CERES causes these "raw" statistics to be over-weighted at higher latitudes; the poles are more frequently visited is a given point at the equator. In Table 3 we compare both untuned computed fluxes (CRS) and tuned with observations (SSF).

The LW parameters (broadband OLR and the window flux) are simulated quite well. More detailed analysis (not shown) reveals some fortuitous compensation of day and night biases. The bias for reflected SW is systematic, and the standard deviation on a footprint by footprint basis is large – over 20 Wm-2. Rutan et al. (2004) thoroughly describes the validation with surface observations.

Table 3   Global comparison of computed and observed fluxes at TOA. Bias as untuned calculation minus observation.   Standard deviation in parenthesis.

TOA flux	Jan 01	Jul 01
SW reflected (Wm-2)		
Observed	253	223
Untuned bias	7 (23)	6 (22)
Tuned bias	1 (11)	2 (10)
OLR (Wm-2)		
Observed	223	229
Untuned bias	0 (8)	0 (8)
Tuned bias	0 (4)	0 (4)
Window 8-12um		
Observed	57	61
Untunted bias	1 (4)	1 (4)
Tuned bias	1 (2)	1 (2)

8 COMPARISON WITH CLAMS

Here we compare an "off line" run of the Langley Fu-Liou radiative transfer code with observations of SW at the surface and TOA which we collected in the CLAMS field campaign. While CLAMS (Smith et al., 2004) conentrated on aerosol effects in cloud-free condistions, we include cloud effects observed by MODIS in the first part of this section. The Fu-Liou code here does not use the Kato et al. formuation for the statistical distribution of cloud optical depth. Cloud effects are instead explicit: Up to 13 different cloud optical depths (yielding up to 13 computed TOA fluxes) are used to simulate a single CERES footprint.   The special CERES scan pattern in CLAMS (July-August 2001) produced multiple views of the target COVE sea platform at different angles on a single day. Precipitable water is taken from local COVE GPS measurements.

"A" calculations in Table 4 use MODIS AOT, and single scattering albedo and asymmetry factor from MATCH (as per OPAC optical properties, noted earlier). "B" calculations in Table 4 use the surface-based AERONET Cimal photometer (Holben et al. 1998) for AOT but retrains MATCH (plus OAPC) for optical properties. "C" takes AOT and optical properties from MATCH (plus OPAC).

Table 4   Fluxes for 248 CERES footprints in CLAMS. Bias as computed – observed.

	Flux in Wm-2 (Std. Dev.)	Aerosol forcing
TOA		
Observed	154	
A bias	11 (31)	13
B bias	8 (32)	10
C bias	16 (29)	18
Surface		
Observed	824	
A bias	-13 (78)	-19
B bias	-7 (83)	-14
C bias	-29 (116)	-23

Clouds were not extensive, but they here nearly double the reflected SW at TOA. The mean biases in Table 4 are comparable to the aerosol forcings. In this case, the small effect of aerosol is masked by the effect of clouds; and by sunglint, which was ubiquitous for the high sun (summer) and low wind conditions of CLAMS.   The generous multi-angle CERES CLAMS sampling yieled many broadband footprints for which clouds were retrieved by the fixed scanning MODIS at different angles; if both instruments used nearly the same angle (as is the general case), errors due to glint could falaciously cancel at TOA. Insolation biases at many land sites are less (Rutan et al., 2004).

Figure 5 shows the superlative performance of the code for diurnal surface insolation with low AOT. Minute by minute time series screened for cloud-free conditions. With no clouds (and no satellite data in Figures 5 and 6), sunglint caused no confusion to inputs. In the third calculation of Figs. 5-6, the inverted single scattering albedo and asymmetry factor from Level 1.5 (thin AOT) and Level 2.0 (thick AOT) products (Dubovik et al., 2001) is used. There is no significant bias in clear sky insolation for other days with low AOT. On a day (Fgure 6) with more aerosol (and the largest absorption in CLAMS), computing aerosol forcing is more problematic.

9 REFERENCES

Augustine, J. A., J. J. DeLuisi, and C. N. Long, 2000: SURFRAD - A national surface radiation budget

network for atmospheric research. Bull. Amer. Meteor. Soc., 81, 2341-2358.

Charlock, T. P., and T. L. Alberta, 1996: The CERES/ARM/GEWEX Experiment (CAGEX) for the retrieval of radiative fluxes with satellite data. Bull. Amer. Meteor. Soc., 77, 2673-2683.

Charlock, T. P., F. G. Rose, and D. A. Rutan, 2001: Aerosols and the Residual Clear-Sky Insolation Discrepancy. Eleventh ARM Science Team Meeting Proceedings (Atlanta, 19-23 March 2001). 15 pp. Available at www.arm.gov under "Publications".

Charlock, T. P., F. G. Rose, and D. A. Rutan, 2003: Validation of the Archived CERES Surface and Atmosphere Radiation Budget (SARB) at SGP. Thirteenth ARM Science Team Meeting Proceedings (Broomfield, Colorado, March 31 – April 4, 2003). Available at www.arm.gov under "Publications".

Charlock, T., F. Rose, D. Rutan, L. Coleman, B. Baum, and R. Green, 1997: The total-sky, global atmospheric radiation budget from radiative transfer calculations using ERBE, AVHRR, and sounding data. Proceeding of the Ninth Conference on Atmospheric Radiation, Long Beach (Feb. 2-7, 1997), AMS, 60-63.

Charlock, T. P., F. G. Rose, D. A. Rutan, T. L. Alberta, D. P. Kratz, L.H. Coleman, G. L. Smith, N. Manalo-Smith, and T. D. Bess, 1997: Compute Surface and Atmospheric Fluxes (System 5.0), CERES Algorithm Theoretical Basis Document. 84 pp. See http://asd-www.larc.nasa.gov/ATBD.

Charlock, T. P., F. G. Rose, D. A. Rutan, D. P. Kratz, Z. Jin, L. H. Coleman, and Q. Fu, 2002: Relationship of Tropical Circulation and Energetics using Retrieved Surface and Atmospheric Radiation Budget for January-August 1998. Extended abstract for 11th Conference on Atmospheric Radiation (AMS), 3-7 June 2002 in Ogden, Utah. http://www-cave.larc.nasa.gov/cave/

Charlock, T. P., F. G. Rose, D. A. Rutan, C. K. Rutledge, L. Larman, Y. Hu, S. Kato, and M. Haeffelin, 2000: Surface and Atmospheric Radiation Budget (SARB) Validation Plan for CERES Subsystem 5.0. 52 pp. See http://asd-www.larc.nasa.gov/validation/valid_doc.html.

Chou, M.-D., and M. J. Suarez, 1999: A solar radiation parameterization for atmospheric studies. NASA/TM-1999-104606, Vol. 15, 40 pp.

Collins, W. D., P. J. Rasch, B. E. Eaton, B. V. Khattatov, J.-F. Lamarque, and C. S. Zender, 2001: Simulating aerosols using a chemical transport model with assilimiation of satellite aerosol retrievals: Methodology for INDOEX. J. Geophys. Res., 106, 7313-7336.

d'Almeida, G., P. Koepke, and E. P. Shettle, 1991: Atmospheric Aerosols - Global Climatology and Radiative Characteristics. A. Deepak Publishing, Hampton, Virginia. 561 pp.

Dickinson, R. E., 1983: Land surface processes and climate - Surface albedos and energy balance. Advances in Geophysics, 25, 305-353.

Dubovik, O., B. Holben, T. Eck, A. Smirnov, Y. Kaufman, M. King, D. Tanre, and I. Slutsker, 2002: Variability of absorption and optical properties of key aerosol types observed in worldwide locations. J. Atmos. Sci., 59, 590-608.

Fillmore, D. W., W. D. Collins and A. J. Conley, 2004: Aerosol direct radiative forcing - estimates from a global aerosol climatology constrained by MODIS assimilation, in preparation.

Fu, Q., W.B. Sun, and P. Yang, 1999: Modeling of scattering and absorption by nonspherical cirrus ice particles at thermal infrared wavelengths. J. Atmos. Sci., 56, 2937-2947.

Fu, Q., and K.-N. Liou, 1993: Parameterization of the radiative properties of cirrus clouds. J. Atmos. Sci., 50, 2008-2025.

Fu, Q., K. Liou, M. Cribb, T. Charlock, and A Grossman, 1997: On multiple scattering in thermal infrared radiative transfer. J. Atmos. Sci., 54, 2799-2812.

Haeffelin, M., S. Kato, A. M. Smith, K. Rutledge, T. Charlock, and J. R. Mahan, 2001: Determination of the thermal offset of the Eppley Precision Spectral Pyranometer. Appl. Opt., 40, 472-484.

Hess, M., P. Koepke, and I. Schult, 1998: Optical Properties of Aerosols and Clouds: The software package OPAC. Bull. Amer. Meteor. Soc., 79, 831-844.

Holben, B. N., T. F. Eck, I. Slutsker, D. Tanre, J. P. Buis, A. Setzer, E. Vermote, J. A. Reagan, Y. J. Kaufman, T. Nakajima, F. Lavenu, I. Jankowiak, and A. Smirnov, 1998: AERONET - A federated instrument network and data archive for aerosol characterization. Remote Sens. Environ., 66, 1-16.

Hu, Y. X., and K. Stamnes, 1993: An accurate parameterization of the radiative properties of water clouds suitable for use in climate models. J. of Climate, 6, 728-742.

Jin, Z., T. P. Charlock, and K. Rutledge, 2002: Analysis of broadband solar radiation and albedo over the ocean surface at COVE. J. Ocean. Atmos. Tech., 19, 1585-1601.

Jin, Z., and K. Stamnes, 1994: Radiative transfer in nonuniformly refracting layered media: Atmosphere-ocean system. Appl. Opt., 33, 431-442.

Jin, Z., K. Stamnes, W. F. Weeks, and S. C. Tsau, 1994: The effects of sea ice on the solar energy budget in the atmosphere-sea ice-ocean system: A model study. J. Geophys. Res., 99, 25,281-25,294.

Kato, S., T. P. Ackerman, E. E. Clothiaux, J. H. Mather, G. R. Mace, M. Wesley, F. Murcray, and J. Michalsky, 1997: Uncertainties in modeled and measured clear-sky surface shortwave irradiances. J. Geophys. Res., 102, 25,881-25,898.

Kato, S., T. P. Ackerman, E. G. Dutton, N. Laulainen, and N. Larson, 1999: A comparison of modeled and measured surface shortwave irradiance for a molecular atmosphere, J. Quant. Spectrosc. Radiat. Transfer., 61, 493-502.

Kato, S., F. G. Rose, and T. P. Charlock, 2004: Computation of domain-averaged irradiance using satellite-derived cloud properties. In press for Journal of Atmospheric and Oceanic Technology.

Kratz, D. P., and F. G. Rose, 1999: Accounting for molecular absorption within the spectral range of the CERES window channel. J. Quant. Spectrosc. Radiat. Transfer, 48, 83-95.

Minnis, P., D. F. Young, D. P. Kratz, J. A. Coakley, Jr., M. D. King, D. P. Garber, P. W. Heck, S. Mayor, and R. F. Arduini, 1997: Cloud optical property retrieval. (System 4.3), CERES Algorithm

Theoretical Basis Document. 60 pp. See http://asd-www.larc.nasa.gov/ATBD.

Minnis, P., D. F. Young, B. A. Wielicki, D. P. Kratz, P. W. Heck, S. Sun-Mack, Q. Z. Trepte, Y. Chen, S. L. Gibson, and R. R. Brown: 2002: Seasonal and Diurnal Variations of Cloud Properties Derived from VIRS and MODIS Data. Extended abstract for 11th Conference on Atmospheric Radiation (AMS), 3-7 June 2002 in Ogden, Utah.

Ohmura, A., H. Gilgen, H. Gegner, G. Muller, M. Wild, E. G. Dutton, B. Forgan, C. Frohlich, R. Philipona, A. Heimo, G. Konig-Langlo, B. McArthur, R. Pinker, C. H. Whitlock, K. Dehne, 1998: Baseline Surface Radiation Network (BSRN/WCRP): New precision radiometry for climate research. Bull. Amer. Meteoro. Soc., 79, 2115-2136.

Rose, F. G., and T. P. Charlock, 2002: New Fu-Liou Code Tested with ARM Raman Lidar and CERES in pre-CALIPSO Exercise. Extended abstract for 11th Conference on Atmospheric Radiation (AMS), 3-7 June 2002 in Ogden, Utah. http://www-cave.larc.nasa.gov/cave/

Rose, F., T. Charlock, D, Rutan, and G. L. Smith, 1997: Tests of a constrainment algorithm for the surface and atmospheric radiation budget. Proceedings of the Ninth Conference on Atmospheric Radiation, Long Beach (Feb. 2-7, 1997), AMS, 466-469.

Rutan, D., and T. Charlock, 1997: Spectral reflectance, directional reflectance, and broadband albedo of the Earth's surface. Proceedings of the Ninth Conference on Atmospheric Radiation, Long Beach (Feb. 2-7, 1997), AMS, 466-469.

Rutan, D., and T. Charlock, 1999: Land surface albedo with CERES broadband observations. Proceedings of the Tenth Conference on Atmospheric Radiation, Madison WI (28 June - 2 July), 1999, AMS, 208-211.

Rutan, D. A., T. P. Charlock, and F. G. Rose, 2002: Closing SW and LW Fluxes Inferred From CERES/SARB at the Top and Bottom of the Atmospheric Column. Extended abstract for 11th Conf. on Atmospheric Radiation (AMS), Ogden, Utah 3-7 June 2002. http://www-cave.larc.nasa.gov/cave/

Rutan, D. A., F. G. Rose, N. Smith, and T. P. Charlock, 2001: Validation Data Set for CERES Surface and Atmospheric Radiation Budget (SARB). GEWEX News, Vol. 11, No. 1 (February), pp. 11-12. Available at http://www.gewex.com under "Newsletter".

Rutan, D. A., T. P. Charlock, F. G. Rose, and J. Madigan, 2003: Surface Albedo at ARM SGP from Helicopter Observations. Thirteenth ARM Science Team Meeting Proceedings, Broomfield, Colorado (30 March – 4 April, 2003). Available at www.arm.gov.

Smith, W. L. Jr., T.P. Charlock, R. Kahn, J.V. Martins, L.A. Remer, P.V. Hobbs, J. Redemann, C.K. Rutledge, 2004: EOS-TERRA aerosol and radiative flux validation: An overview of the Chesapeake Lighthouse and Aircraft Measurements for Satellites (CLAMS) experiment. Accepted by J. Atmos. Sci.

Stokes, G. M., and S. E. Schwartz, 1994: The Atmospheric Radiation Measurement Program (ARM) Program: Programmatic Background and Design of the Cloud and Radiation Test Bed. Bull. Amer. Meteor. Soc., 75, 1201-1221.

Tegen, I., and A. A. Lacis, 1996: Modeling of particle size distribution and its influence on the radiative properties of mineral dust aerosol. J. Geophys. Res., 101, 19,237-19,244.

Wielicki, B. A., B. R. Barkstrom, E. F. Harrison, R. B. Lee, G. L. Smith, and J. E. Cooper, 1996: Clouds and the Earth's Radiant Energy System (CERES): An Earth Observing System Experiment. Bull. Amer. Meteor. Soc., 77, 853-868.

Wilber, A. C., D. P. Kratz, and S. K. Gupta, 1999: Surface emissivity maps for use in satellite retrievals of longwave radiation, NASA TP 1999-209362, 35 pp.

Yang, S.-K., S. Zhou, and A. J. Miller, 2000: SMOBA: A 3-dimensional daily ozone analysis using SBUV/2 and TOVS measurements. http://www.cpc.ncep.gov/products/stratosphere/SMOBA/smoba_doc.html
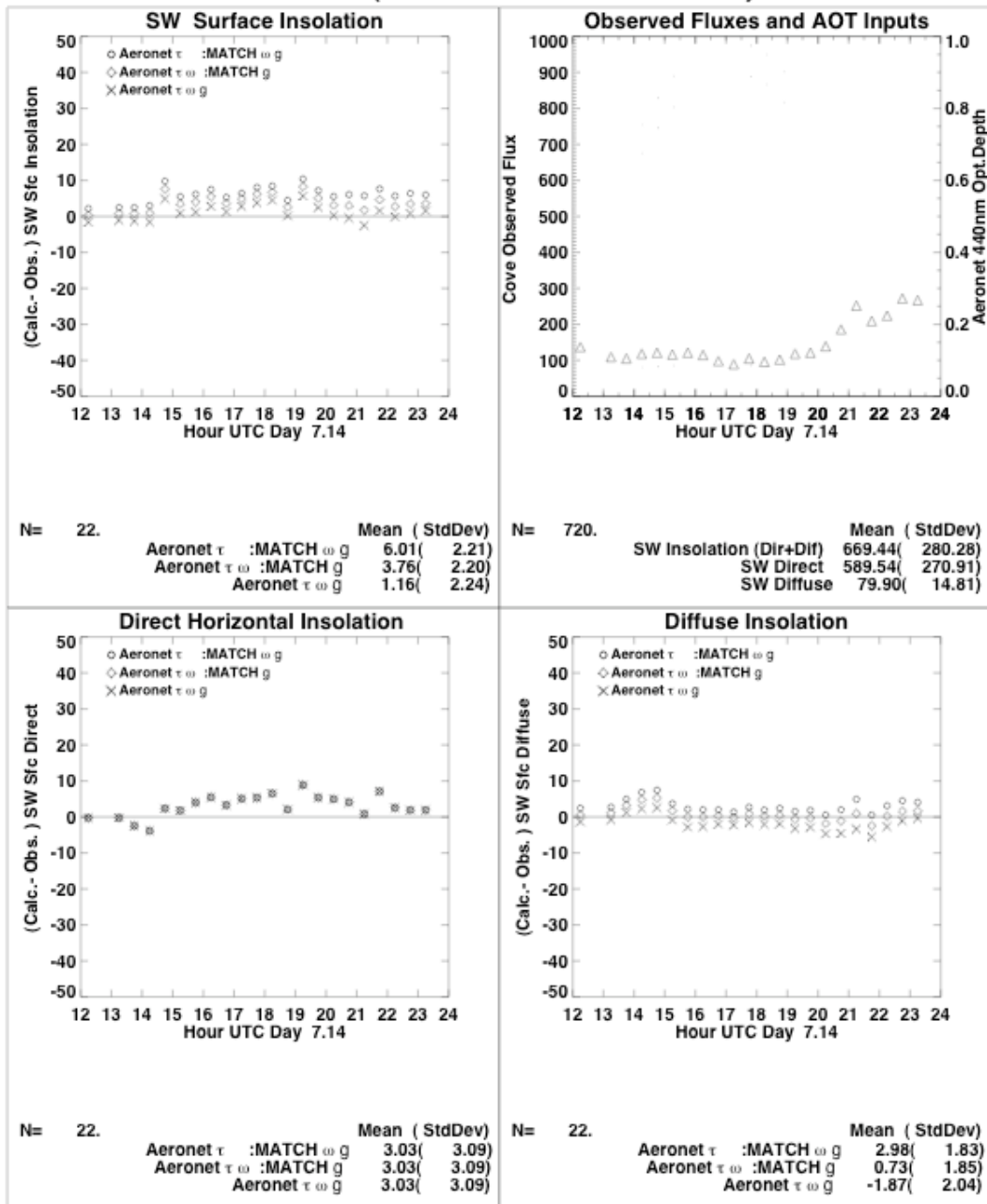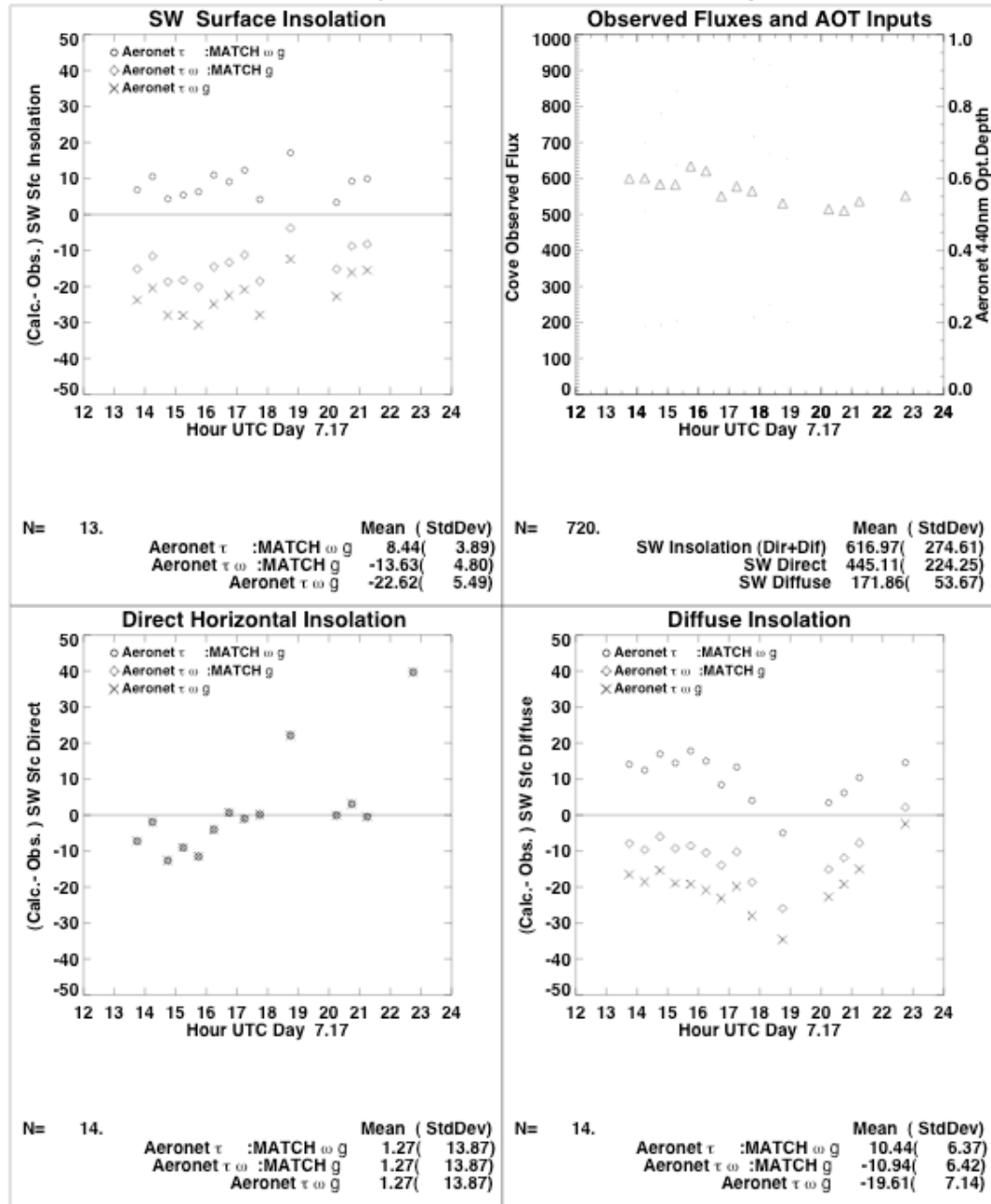
Figure 5. Bias (calculated minus observed) for surface flux on a clear day (14 July 2001) at the COVE sea platform. Thin dots in upper right panel show observed insolation Calculation 1 uses AERONET AOT and MATCH (plus OPAC) for SSA and g. Calculation 2 uses AERONET for AOT and ssa. Calculation 3 uses AEONET for all parameters.

Figure 6. Bias (calculated minus observed) for surface flux on a more turbid day (17 July 2001) at the COVE sea platform. Thin dots in upper right panel show observed insolation. Calculation 1 uses AERONET AOT and MATCH (plus OPAC) for SSA and g. Calculation 2 uses AERONET for AOT and ssa. Calculation 3 uses AEONET for all parameters.